Numerical Investigation of Lightweight Design and Performance Analysis of Rubber-Wheeled Rail Track Inspection Car

Paramust Juntarakod*, Viroch Sukontanakarn, Paanthong Sroymuk, and Tanawat Chalardsakul

Faculty of Engineering, Rajamangala University of Technology Isan, Khon Kaen, Thailand
Email: paramust.ju@rmuti.ac.th (P.J.); viroch.su@rmuti.ac.th (V.S.); paanthong.sr@rmuti.ac.th (P.S.); tanawat.ca@rmuti.ac.th (T.C.)
*Corresponding author

***Abstract*—This research introduces a novel lightweight steel frame and rubber-wheeled system for a small, four-wheeled vehicle without suspension or differential, designed to replace traditional railway inspection cars that use heavy steel wheels. The study aimed to model and perform a static analysis of a chassis constructed with circular beams. Modeling and analysis were conducted using the finite element analysis capabilities of ANSYS. In this research, we analyzed the materials AISI 1020 and structural steel to determine the strength, von-Mises stress, and total deformation of the body frame. The focus was on evaluating the frame's response to force loads and deflection under varying load conditions. The analysis results were validated through a comparative assessment with numerical results and confirmed to be safe for impact loading. Following this, all components and equipment for the rail track inspection car were meticulously constructed and assembled. The strength analysis of the body frame met the initial design objectives, demonstrating its effectiveness for use as a rail track inspection car. The successful completion of this analysis validates its suitability for practical deployment in railway inspection tasks, contributing to operational efficiency and maintenance effectiveness in rail infrastructure management.**

***Keywords*—rail track inspection car, finite element analysis, rubber-wheeled, steel frame, ANSYS software, factor of safety**

I. Introduction

At present, Thailand has developed rail transportation systems on many routes. Studies have been conducted on the design of various types of railway systems, including double-track designs. The future high-speed trains in Thailand will have railway routes that extend many kilometers. Consequently, there must be regular maintenance of the tracks [1] using track inspection vehicles as part of the Railway Maintenance System of the State Railway of Thailand. For repair and maintenance, staff will ensure the tracks are safe and ready for use at all times. However, the current rail inspection vehicles are heavy and can only operate over short distances.

The chassis design of the rail track inspection car must support the weight of the operator, engine, and other systems. It needs to be strong and capable of withstanding all forces acting on it. Therefore, the selection of steel pipe material [2] must consider the appropriate length and diameter while being as lightweight [3] as possible. The advantages of this chassis design include full protection for the driver, the required strength and torsional rigidity, and reduced weight, which in turn lowers costs. This study analyzes chassis design stress using finite element analysis [4–6] to provide useful and cost-effective simulation data for design improvement.

Chassis manufacturers must consider structural integrity during the design process to prevent failure while optimizing material usage [7]. The rail track inspection car used for checking road conditions consists of a diesel engine and is called the “TOK Car” in Thailand. The vehicle is made of steel, painted yellow, and has four steel wheels, as shown in Fig. 1 below:

Fig. 1. The old rail track inspection car.

The chassis of the rail track inspection car has been designed similarly to that of a go-kart, leveraging the simplicity and robustness of go-kart designs [8–10]. One of the primary advantages of employing static analysis in this context is that it eliminates the need to simulate dynamic variations in force values, simplifying the analysis process and reducing computational

Manuscript received April 2, 2024; revised June 16, 2024; accepted June 25, 2024; published November 8, 2024.

doi: 10.18178/ijmerr.13.6.566-572

complexity [11]. The go-kart design process, from initial conceptualization to CAD modeling and analysis, utilizes tools such as SolidWorks for design and ANSYS program for structural analysis [12, 13]. The Budd-Michelin rubber-tired rail cars were built by the Budd Company in the United States between 1931 and 1933 using the French firm Michelin's "Michelin" rail car design. The Budd Company built four production rubber-tired rail cars for American railroads [14]: one for the Reading Company, two for the Pennsylvania Railroad, and the Silver Slipper for the Texas and Pacific Railway. Rubber-tired rail cars achieved greater success in France, as Michelin built 30 for the Eastern Railway of France in 1937. Furthermore, similar rubber-tired subway cars have been adopted in Canada and Mexico as well as on numerous systems in Europe. Currently, rubber-tired rail cars are not used because rubber on train wheels reduces traction with the steel rails. Steel on steel provides better traction, especially in adverse weather conditions like rain or snow. Rubber would not grip the steel rails as effectively, potentially leading to slippage and safety issues. Additionally, rubber is not as durable as steel. Train wheels need to withstand significant wear and tear, especially when pulling heavy loads up inclines. This paper presents a novel design for a rail track inspection car, which features rubber-wheeled and a lightweight steel chassis. The primary objective of this design is to develop an inspection car capable of easily moving and lifting off the rail, or quickly changing its driving direction [15]. The main purpose of this innovation is to facilitate the inspection of railway track conditions [16], providing operators with essential information for track maintenance. This new design aims to replace traditional rail inspection vehicles that are equipped with heavy steel wheels, thus offering a more efficient and versatile solution. This article presents a lightweight rail inspection vehicle with rubber tires for short-distance railway track inspections. It is designed with a lightweight steel structure that can carry two people along with luggage, tools, and equipment with a total weight not exceeding 300 kg. The vehicle can be lifted to change direction on the railway tracks.

The remainder of the paper is organized as follows. The materials and methods are explained in Section II. Section III is the result and discussion. Finally, the main conclusion is drawn in Section IV.

II. Materials and Methods

The experimental method outlined in this paper is divided into two distinct phases. The first phase involves the selection and simulation of the chassis model. In the second phase, the focus shifts to selecting and simulating the rubber-wheeled.

A. Model and Simulation of Frame Body

1) Material selection

The chassis is constructed using AISI-1020 tube steel, a medium carbon steel selected for its favorable properties, including high tensile strength, ductility, light weight, and improved weld ability. The properties of the AISI-1020 material are detailed in Table I. Fig. 2 illustrates the 3D modeling of the frame design.

TABLE I. The AISI-1020 Material Properties

Property	Value
Modulus of elasticity	205 GPa
Density	7870 g/mm^3
Poisson ratio	0.29
Yield strength	350 MPa
Tensile strength	420 MPa

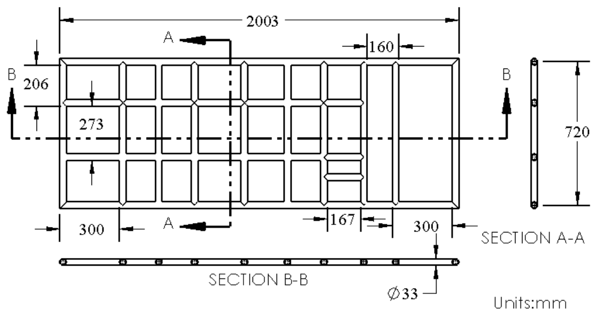

Fig. 2. The drawing model of chassis.

Table II shows the specification of pipe steel for the construction of the frame.

TABLE II. Specification of Frame Pipes

Parameter	Value
Dimension of pipes	25.4 mm diameter and 2.3 mm thickness
Mass of frame	12.291 kg
Welding type	Electric arc welding
Total length of pipe for used	12,000 mm

2) Methodology

The overall study flow chart outlines the main objective of the study, which is to determine the maximum deflection of the chassis of the rail track inspection car under static conditions. This process is illustrated in Fig. 3.

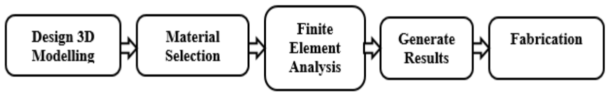

Fig. 3. The study flow chat of finite element analysis.

For the purpose of finite element analysis [17, 18], certain tests were conducted on the chassis to calculate the impact load [19]. Table III presents the distribution of the weight of the rail track inspection cars.

TABLE III. Distribution of Weight

Parameter	Value
Weight of the rail track inspection car	70 kg
Weight of the two driver	180 kg
Misc. weight (fuel, tools, etc.)	50 kg

3) Front impact test

The equation for calculating the impact force can be derived from the basic principles of physics involving force, mass, and change in velocity. The basic equation is shown in Eq. (1).

$$F = \frac{mg\Delta\upsilon}{\Delta t} \qquad (1)$$

where: F is the impact force, m is the mass of the object, υ is the change in velocity (final velocity minus initial velocity), and $\mathrm{V}t$ is the time duration over which the change in velocity occurs. The equation for FOS is shown in Eq. (2).

$$FOS = \frac{Yield\ strength\ of\ AISI1020}{Mises\ Stress} \qquad (2)$$

In this case, if the mass of the object is 300 kg and the velocity changes from 5–40 km per hour to 0 in 0.1 s. The results are shown in Table IV.

TABLE IV. SUMMARIZING OF VELOCITY AT IMPACT FORCE

Velocity (km/hr)	Impact force (N)	Max. Deformation (mm)	Max. Mises Stress (MPa)	FOS
5 (1.389 m/s)	4,167	73.041	28.056	12.5
10 (2.778 m/s)	8,334	146.08	56.113	6.24
15 (4.167 m/s)	12,500	219.11	84.163	4.16
20 (5.556 m/s)	16,680	292.37	112.31	3.12
30 (8.333 m/s)	25,000	438.201	168.33	2.08
40 (11.11 m/s)	41,640	584.22	224.41	1.56

We would like to provide an example of the test results for the impact force while moving at a velocity of 20 kilometers per hour as follows. The front impact analysis at velocity of 20 km/h was carried out on the ANSYS R16.2

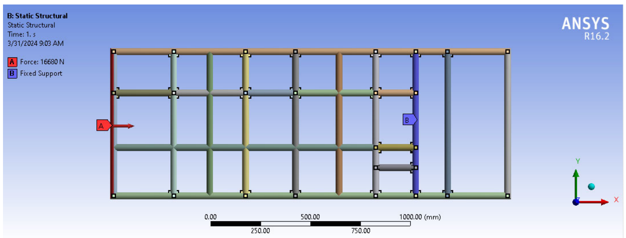

Fig. 4. Fixed and force support.

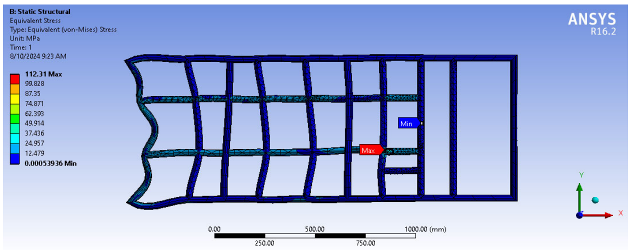

Fig. 5. Stress parameters of front impact.

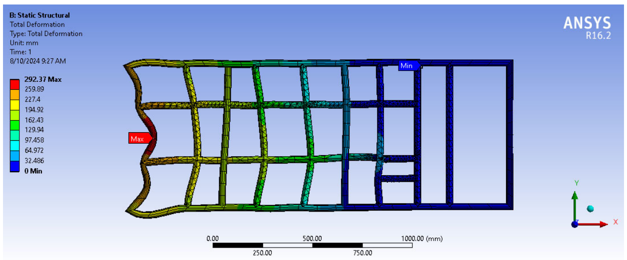

Fig. 6. Total deformation parameters of front impact.

In the simulation study, Fig. 4 demonstrates the application of fixed and force support conditions on the chassis model. Specifically, a front impact force of 16,680 N was applied to the front frame of the chassis. Fig. 5 shows the stress distribution within the chassis resulting from the impact.

Fig. 6 depicts the total deformation experienced by the chassis under the same conditions. The analysis revealed a maximum deformation of 292.37 mm in the chassis structure. This deformation is considered acceptable according to the criteria established in Eq. (2). The FOS for front impact on the chassis is calculated to be 3.12, as illustrated in Fig. 7.

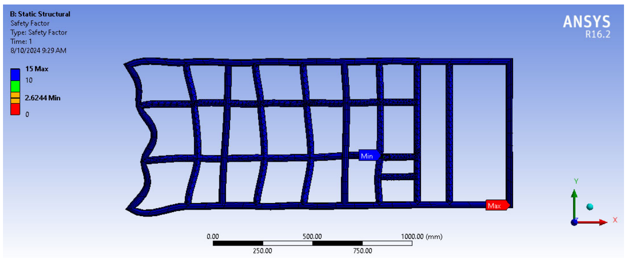

Fig. 7. FOS parameters of front impact.

4) The chassis impact test

As for the chassis rail inspection vehicle is designed to be the right size for two operators and lightweight. Therefore, the strength of the materials used to make the chassis for a rail track inspection car was analyzed using ANSYS 16.2 software. In this case, if the object's mass is 80–400 kg, the remote force was applied to the frame with four four-position frame fixes, thus the remote force was distributed to the frame chassis as divided by four. The results are shown in Table V.

TABLE V. SUMMARIZING OF TOTAL WEIGHT AT FORCE SUPPORT

Total weight (kg)	Force support (N)	Max. Deformation (mm)	Max. Mises Stress (MPa)	FOS
80	196.25	13.89	20.07	17.4
120	294.25	20.83	30.10	11.6
150	368	26.05	37.64	9.29
200	490.5	34.73	50.17	6.97
250	613.25	43.417	62.73	5.58
300	735.75	52.09	75.26	4.65
400	981	69.45	100.34	3.49

In this case, we are specifying the design to have a mass of 300 kg. In Table III, the total weight is shown as 300 kg (735.75 N).

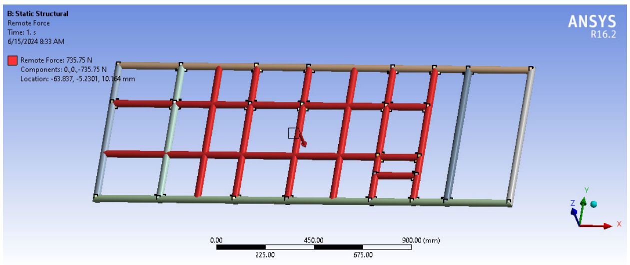

Fig. 8. Fixed and force support for chassis.

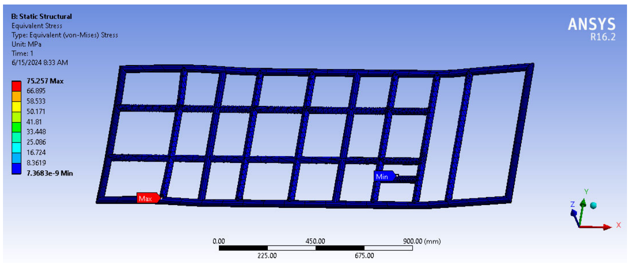

Fig. 9. Stress parameters of chassis impact.

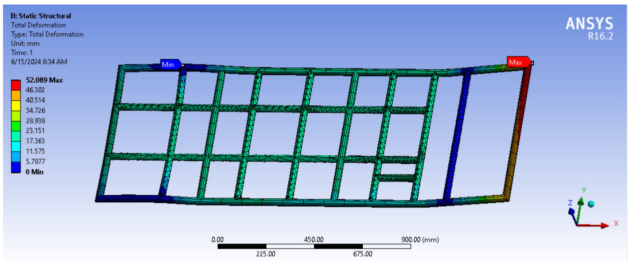

Fig. 10. Total deformation parameters of chassis impact.

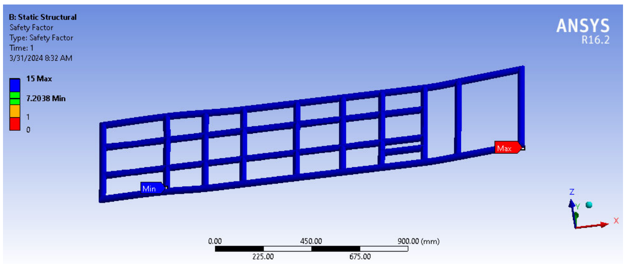

Fig. 11. FOS parameters of body impact.

Fig. 8 shows the configuration of the chassis model with fixed and force support conditions. This likely illustrates how the chassis is supported and where the force is applied. Fig. 9 displays the stress distribution across the chassis model when subjected to the applied force. This helps in understanding where the maximum stresses occur. Fig. 10 shows the total deformation (displacement) of the chassis model due to the applied force. It indicates the magnitude and distribution of displacements within the chassis structure. The Factor of Safety for chassis impact is calculated to be 3.49. This FOS value indicates the margin of safety the chassis has before reaching its yield or failure point under the impact condition. Fig. 11 presents a summary or assessment of the results, confirming that the maximum deformation of 52.09 mm is within acceptable limits. This conclusion is based on comparing the obtained results against design criteria or standards. In summary, the simulation results suggest that the chassis model withstands the applied force adequately. The maximum deformation observed (52.09 mm) and the calculated Factor of Safety (3.49) indicate that the chassis design meets or exceeds the required performance criteria under the impact condition evaluated. This information is crucial for ensuring the structural integrity and reliability of the chassis in real-world applications.

B. Modelling and Simulation of Rubber Wheel and Rim

1) Model of rubber and rim

The rubber wheel being discussed is the DEESTONE type D191. Its dimensions are 271 mm in diameter and 127 mm in width. These dimensions are standard specifications for this particular type of rubber wheel. Fig. 12 plays a crucial role in visually conveying the physical attributes and design specifics of the rubber wheel under study. This visual aid enhances the reader's comprehension and serves as a reference point for discussions and analyses presented in the paper.

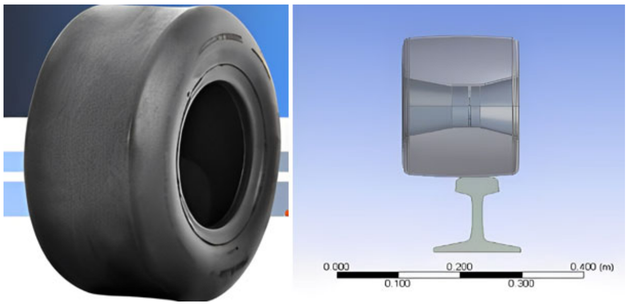

Fig. 12. Real and drawing and of rubber-wheeled model with rim model.

2) Engineering data

In the ANSYS Workbench 16.2 software, select and drag the static structural elements [20] into the red dotted loop. Then, select the engineering data and set the materials for the rim and rubber-wheeled [21] as shown in Table VI.

TABLE VI. MATERIAL PROPERTIES

Property	Rubber wheel (Polyethylene)	Rim (Aluminum alloy)	Rail tracks (Steel)
Dimension	271×127mm	127×133.35mm	0.5m
Density	1950 kg/mm^3	2,770 kg/mm^3	7,850 kg/mm^3
Co-eff. of Thermal Expansion	0.00023 C^{-1}	0.000023 C^{-1}	0.000012 C^{-1}
Young's Modulus	1,100 MPa	71,000 MPa	200,000 MPa
Yield strength	25 MPa	280 MPa	250 MPa
Tensile Ultimate strength	33 MPa	310MPa	460 MPa

In summary, the rubber wheels made of polyethylene are designed to operate effectively at an air pressure of 20 psi (137,895 Pa). They support the car's weight while rolling along the track. The aluminum alloy rims provide structural support and secure the rubber wheels in place. These specifications are crucial for ensuring the reliability and performance of rail track inspection cars during their operational tasks.

TABLE VII. WEIGHT AT AIR PRESSURE OF 20 PSI

Weight for one wheel (kg)	Force support (N)	Max. Deformation (mm)	Max. Mises Stress (MPa)	FOS
25	245	1.063	2.19	11.42
30	294	1.276	2.62	9.54
45	441	1.914	3.93	6.36
55	540	2.344	4.82	5.19
60	589	2.556	5.25	4.76
75	736	3.194	6.56	3.81
85	834	3.62	7.44	3.36
100	981	4.26	8.75	2.86

In summary, Table VII provides essential weight data for one wheel under specific air pressure conditions, aiding engineers in designing and analyzing the performance of rubber wheels used in rail track inspection cars. This information is fundamental for ensuring operational safety, efficiency, and durability of the vehicles during their inspection tasks. The described process involves preparing and importing vehicle geometry for simulation, ensuring load distribution among wheels, and utilizing tire tread models to analyze and optimize the vehicle's performance and durability. This approach integrates detailed geometry handling with advanced simulation techniques to achieve reliable engineering outcomes.

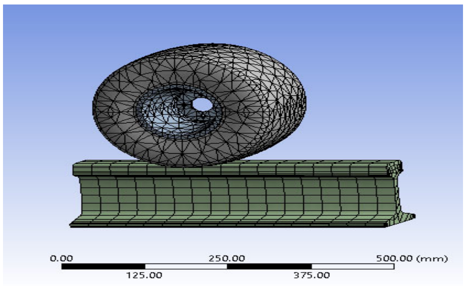

Fig. 13. The rubber wheel mesh.

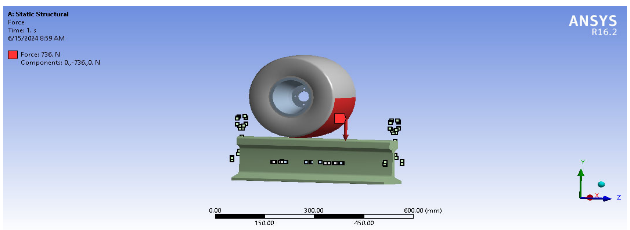

Fig. 14. The fixed support and applied force.

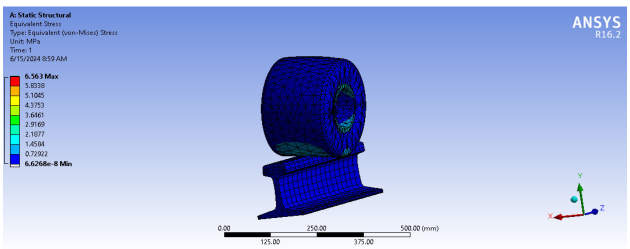

Fig. 15. Stress parameters of the rubber wheels.

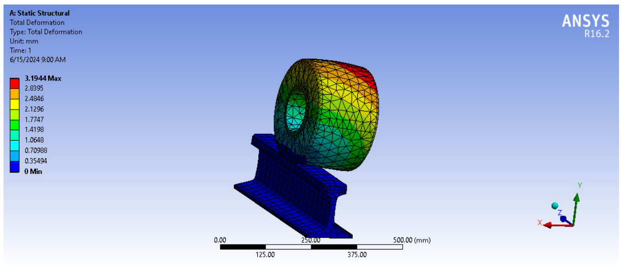

Fig. 16. Total deformation parameters of the rubber wheels.

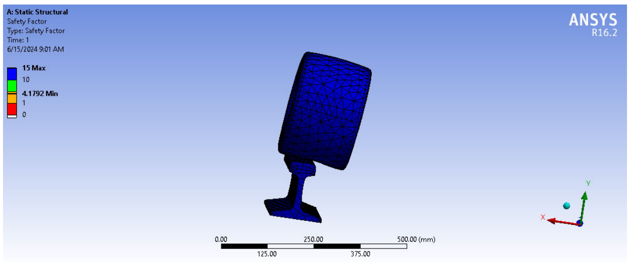

Fig. 17. FOS parameters of the rubber wheels.

Fig. 13 illustrates the meshing process applied to the rubber-wheeled chassis model. Meshing involves dividing the geometry into small elements to facilitate accurate numerical simulation. A well-structured mesh is crucial for obtaining reliable results in Finite Element Analysis (FEA) simulations, ensuring both computational efficiency and accuracy. Fig. 14 shows the setup of the chassis model under simulation conditions. It indicates how the chassis is supported (fixed and force supports) and where the force is applied. The force support conditions are essential for replicating real-world scenarios where external forces act on the chassis, such as during vehicle operation or impact events. Fig. 15 presents the results of stress distribution across the chassis model when subjected to the applied force (736 N on one rubber wheel). Stress simulation helps in identifying critical areas where the chassis experiences high stress concentrations, which are crucial for assessing potential failure points or areas requiring reinforcement. Fig. 16 displays the total deformation (displacement) of the chassis model due to the applied force. Deformation simulation shows how the chassis structure responds to the force, indicating the magnitude and distribution of displacements within the model. Fig. 17 assesses the maximum deformation observed in the chassis model, which is 3.194 mm due to the applied force of 736 N. The statement confirms that this deformation value falls within acceptable limits, implying that the chassis design meets the required performance criteria under the impact condition evaluated. In summary, these figures collectively depict the simulation and analysis process of a rubber-wheeled chassis model under a specified force condition. They provide insights into stress distribution, deformation behavior, and overall structural response, crucial for validating and optimizing the chassis design for durability and safety in real-world applications.

III. Result and Discussion

The analysis of strength values for various parts of a lightweight rubber wheel rail track inspection car was conducted under a design load of 300 kg using the Finite Element Analysis method. The simulation of the main structure revealed the maximum stress value (von-Mises). At the point of attachment to the shaft, the maximum stress was 75.26 MPa with a FOS of 4.65. Additionally, during a crash test at a velocity of 20 km/h with a weight of 300 kg, further analysis showed that the maximum stress value (von-Mises) occurred in this area, with the maximum stress at the point of attachment to the shaft reaching 112.31 MPa and an FOS of 3.12. Subsequently, the tires and wheel rims underwent testing, with each wheel capable of supporting a weight of 75 kg. During the functional test with a real prototype, various structures were observed to withstand tensile force without damage. Simulation results for the main structure indicated the maximum stress values at the attachment point with the shaft, with a maximum stress value (von-Mises) of 6.56 MPa and an FOS of 3.81. Table VIII summarizes all of the model design analysis.

TABLE VIII. Summarizing of Effect

Element	FOS	Maximum Deformation (mm)	Maximum Stress (MPa)
Front impact at 20 km/h	3.12	292.37	112.31
Chassis impact at weigh of 75 kg/wheel	4.65	52.09	75.26
Rubber-wheeled at weigh of 75 kg/wheel and air pressure 20 psi	3.81	3.194	6.56

Use FEA results to verify and validate the design assumptions and structural integrity of the steel structure. Ensure compliance with applicable codes, standards, and project requirements based on the FEA findings. Based on the verified design from FEA, proceed to detailed design and preparation for fabrication. Prepare detailed drawings, specifications, and instructions for manufacturing the steel structure. The picture referred to likely serves as a visual reference or blueprint for constructing the steel structure, guiding fabrication and assembly processes based on the finalized design and analysis results from FEA.

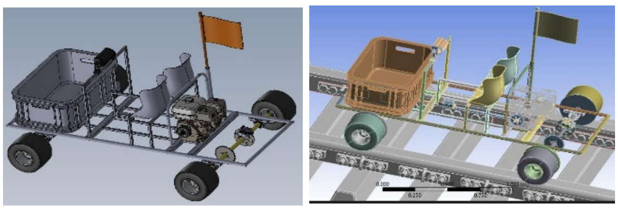

Fig. 18. 3D CAD modelling of rail track inspection cars.

Fig. 19. The rail track inspection cars operating on the rail track.

Fig. 20. The operating on the rail track with two drivers.

Fig. 18 depicts the Computer-Aided Design (CAD) model of the rail track inspection car. It showcases the detailed geometric representation of the car, including its structural components, dimensions, and overall design features. CAD modeling allows engineers to visualize and refine the design before fabrication, ensuring that all components fit together correctly and meet the intended specifications. It aids in identifying potential design issues, optimizing ergonomics, and integrating necessary equipment and features for efficient operation on rail tracks. Fig. 19 illustrates the rail track inspection cars in action on the actual railway tracks. It shows the cars performing their intended function of inspecting and possibly maintaining the railway infrastructure. The image provides insights into how the cars navigate and operate on the rail tracks. Fig. 20 depicts the rail track inspection car in operation with two operators/drivers on board. The presence of two operators suggests that the car may require multiple personnel to manage inspection tasks effectively. Operator's likely work together to monitor equipment, collect data, and ensure safe operation of the vehicle during inspections. Having two drivers can enhance efficiency in data collection and inspection processes while ensuring safety protocols are adhered to during operations on railway tracks.

IV. Conclusion

The research focused on simulating and analyzing impacts and collisions involving a lightweight rail track inspection car model using ANSYS software. The model was tested under various collision conditions, and the resultant deformation and stresses were evaluated at speeds below 20 km/h. The car weighs 50 kg and has dimensions of 1.9 m in length and 0.8 m in width. It is designed to carry a load of up to 300 kg. The analysis confirmed that the steel frame meets the design parameters, demonstrating sufficient strength and structural integrity for effective use as a rail track inspection vehicle. The lightweight design and specified operational capabilities, including speed and load capacity, make it efficient for conducting inspections while ensuring safety and maneuverability on railway tracks. In summary, the design and analysis of the lightweight rail track inspection car align with specific operational needs, emphasizing functionality, safety, and structural robustness. The successful completion of the strength analysis validates its suitability for practical deployment in railway inspection tasks, contributing to operational efficiency and maintenance effectiveness in rail infrastructure management.

Conflict of Interest

The author declared no potential conflicts of interest with respect to the publication of this article.

Author Contributions

P.J. conducted the research; T.C. and P.S. analyzed the data; V.S. wrote the paper; all authors had approved the final version.

Funding

This research was funded by Faculty of Engineering, Rajamangala University of Technology Isan Khon Kaen Campus grant number ENG6/66.

Acknowledgment

The authors would like to thank Department of Mechatronics, Faculty of Engineering, and Rajamangala University of Technology Isan Khon Kaen Campus for providing the laboratory and experimental lab practices for this research.

References

[1] W. Shan and G. Zhao, "Design of multifunctional railway track inspection vehicle," *Journal of Physics: Conference Series*, 2174, 2022.

[2] M. I. Maulana, A. R. Prabowo, T. Muttaqie *et al.*, "Assessment of steel pipe-shaped structure under blast loading: A benchmark and parametric study using finite element approach," *International Journal of Mechanical Engineering and Robotics Research*, vol. 13, no. 1, 2024.

[3] U. Idrees, S. Ahmad, I. A. Shah *et al.*, "Finite element analysis of car frame frontal crash using lightweight materials," *Journal of Engineering Research*, vol. 11, 2023.

[4] K. Bopaiah, "Design and analysis of Go-Kart using finite element method," *International Journal of Science Technology & Engineering*, vol. 4, no. 8, 2018.

[5] M. D. Vijayakumar, C. R. Kannan, S. Manivannan *et al.*, "Finite element analysis of automotive truck chassis," *IOP Conf. Series: Materials Science and Engineering*, 2020.

[6] M. A. Zulkifli, K. S. Basaruddin, Y. A. Rahim, M. Afendi, and P. Gurubaran, "Three dimensional finite element analysis on railway rail," in *Proc. International Conference on Advanced Manufacturing and Industry Applications*, 2018.

[7] A. K. Faizin, R. Rizaldi, W. A. S. Putra, and N. Hasan, "Structural analysis of chassis frame of a prototype car: A finite element method," in *Proc. 4th International Conference Eco-Innovation in Science, Engineering, and Technology*, 2023.

[8] P. K. Jain, P. Yadav, A. Natu *et al.*, "Design, development and fabrication of a Go-Kart," *International Journal of Advance Research and Innovation*, vol. 6, no. 2, pp. 145–161, 2018.

[9] T. Mihalic, J. Hoster, V. Tudic, and T. Kralj, "Concept design and development of an electric Go-Kart chassis for undergraduate education in vehicle dynamics and stress applications," *Appl. Sci.*, vol. 13, 2023.

[10] R. Pathak, D. Joshi, A. Kulkarni *et al.*, "Design and analysis of a Shifter-Kart," *IOSR Journal of Mechanical and Civil Engineering (IOSR-JMCE)*, vol. 14, no. 4, pp. 16–36, 2017.

[11] K. Mateja and K. Zenowicz, "Shaft design for electric Go-Kart," *Technical Sciences*, vol. 25, pp. 5–16, 2022.

[12] D. Sampayo, P. Luque, D. A. Mantaras, and E. R. Rodriguez, "Go-Kart chassis design using finite element analysis and multibody dynamic simulation," *International Journal of Simulation Model*, vol. 20, no. 2, pp. 267–278, 2021.

[13] M. Jha, S. Raut, S. Pokhrel, and N. K. Yadav, "Design and analysis of chassis of four-seater car," *International Journal for Research in Applied Science & Engineering Technology (IJRASET)*, vol. 9, no. 8, 2021.

[14] J. H. White, *The American Railroad Passenger Car*, Baltimore: Johns Hopkins University Press, 1985, pp. 623–624.

[15] S. Muller and M. Blundell, "The testing of pneumatic tyres for the interpretation of tyre behaviour for road/rail vehicles when operating on rails," *Journal of Automobile Engineering*, vol. 237, no. 14, pp. 3275–3284, 2023.

[16] P. Chen, Y. Hu, W.-T. Liand, and P.-J. Wang, "Rail wear inspection based on computer-aided design model and point cloud data," *Advances in Mechanical Engineering*, vol. 10, no. 12, pp. 1–9, 2018.

[17] S. Ramteke and V. Nambiar, "Material selection methodology for a Go-kart chassis using FEA and weighted decision matrices," *Turkish Journal of Computer and Mathematics Education*, vol. 13, no. 2, pp. 539–550, 2022.

[18] J.-J. Kim, M. Bae, M.-P. Hong, and Y.-S. Kim, "Finite element analysis on welding-induced distortion of automotive rear chassis component," *Metals*, vol. 12, no. 287, 2022.

[19] K. Nagendra, G. V. R. Reddy, P. Vijay, K. A. Yadav, and G. N. Reddy, "Design and analysis of a Go-Kart chassis by comparing different materials," *International Research Journal of Modernization in Engineering Technology and Science*, vol. 4, no. 7, pp. 1208–1216, 2022.

[20] M. Ilunga and A. Agarwal, "A finite-element-analysis-based feasibility study for optimizing pantograph performance using aluminum metal matrix composites," *Processes*, vol. 12, no. 445, 2024.

[21] M. K. Sahu, V. Achwal, and S. Sharma, "FEA analysis of tyre tread under loading and unloading condition," *International Journal of Science and Research (IJSR)*, vol. 8, no. 6, 2019.